Where is the Quantum Spin Nematic?

Shengtao Jiang (□□□), Judit Romhányi, Steven R. White, M. E. Zhitomirsky, and A. L. Chernyshev

Phys. Rev. Lett. **130**, 116701 — Published 15 March 2023

DOI: 10.1103/PhysRevLett.130.116701

The Elusive Spin Nematic

Shengtao Jiang (蒋晟韬),[1] Judit Romhányi,[1] Steven R. White,[1] M. E. Zhitomirsky,[2,3] and A. L. Chernyshev[1]

[1] *Department of Physics and Astronomy, University of California, Irvine, California 92697, USA*
[2] *Université Grenoble Alpes, Grenoble INP, CEA, IRIG, PHELIQS, 38000 Grenoble, France*
[3] *Institut Laue-Langevin, 71 Avenue des Martyrs, CS 20156, 38042 Grenoble Cedex 9, France*

(Dated: December 16, 2022)

We provide strong evidence of the spin-nematic state in a paradigmatic ferro-antiferromagnetic J_1–J_2 model using analytical and density-matrix renormalization group methods. In zero field, the attraction of spin-flip pairs leads to a first-order transition and no nematic state, while pair-repulsion at larger J_2 stabilizes the nematic phase in a narrow region near the pair-condensation field. A devil's staircase of multi-pair condensates is conjectured for weak pair-attraction. A suppression of the spin-flip gap by many-body effects leads to an order-of-magnitude contraction of the nematic phase compared to naïve expectations. The proposed phase diagram should be broadly valid.

Introduction.—Liquid crystals—which combine properties of a liquid and a solid that seem mutually exclusive—were considered an exotic state of matter for nearly a century before becoming ubiquitous in technology [1, 2]. Their quantum analogues have been hypothesized and pursued in several contexts, such as electronic nematic states in strongly correlated materials [3–6], spin nematics in frustrated magnets [7–17], and supersolids in He^4 and cold atomic gases [18–21]. Quantum spin nematics are particularly elusive, as they should interpolate between a magnetically ordered spin solid and a spin liquid, another exotic and elusive state [22, 23]. Like spin liquids, spin nematics lack conventional dipolar magnetic order, but instead break spin-rotational symmetry with quadrupolar or higher-rank multipolar ordering [24–26], making their experimental detection challenging [27].

An earlier study has proposed an intuitive view of the nematic states as of the Bose-Einstein condensates (BECs) of *pairs* of spin excitations with a gap in the single-particle sector [26]. In a nutshell, a nematic state occurs if a conventional order due to a BEC of single spin flips [28] is preempted by a BEC of their pairs. Since the bound states (BSs) of magnons in ferromagnets (FMs) do not Bose-condense [29, 30], it was suggested that magnetic frustration can facilitate nematic pair-BEC [26], a concept explored in several classes of frustrated magnets theoretically [31–46] and experimentally [8–17].

One of the simplest paradigmatic models for this scenario is the J_1–J_2 ferro-antiferromagnetic (AFM) $S=1/2$ Heisenberg model on a square lattice in external field,

$$H = J_1 \sum_{\langle ij\rangle_1} \mathbf{S}_i \cdot \mathbf{S}_j + J_2 \sum_{\langle ij\rangle_2} \mathbf{S}_i \cdot \mathbf{S}_j - h \sum_i S_i^z, \qquad (1)$$

where $\langle ij\rangle_{1(2)}$ denotes the first (second) nearest-neighbor bonds, the field $h = g\mu_B H$, $J_1 = -1$ is set as the energy unit, and $J_2 > 0$. The FM is a ground state for small J_2; for large J_2 it is a stripe AFM [47]; see Fig. 1(a).

Prior studies on this model [31–33] have proposed the nematic state to intervene between FM and AFM phases in a broad region similar to the one shown in Fig. 1(a). However, this contradicts the robust numerical evidence of a direct FM-AFM transition in zero field [47], highlighting a common pitfall of claiming the nematic state based on correlations that are subsidiary to a prevalent dipolar order. It also shows that the nematic state of BEC pairs may be superseded by other instabilities.

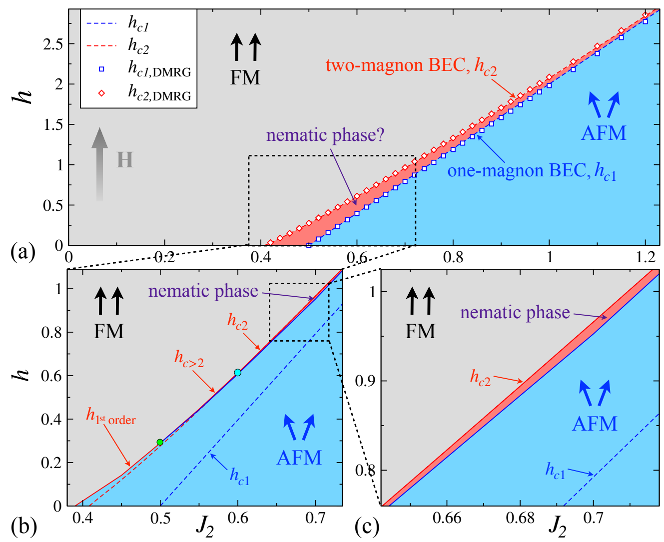

FIG. 1. (a) The naïve h–J_2 phase diagram of model (1) based on the single spin-flip and pair-BEC h_{c1} and h_{c2} lines. Lines and symbols show analytical and DMRG results, respectively. (b) The actual phase diagram of the model (1) in the zoomed region of (a), with the first-order, multi-pair, and pair-BEC transitions emphasized. (c) The zoomed sector of (b) showing the extent of the nematic phase near pair-BEC field.

In this Letter, we combine analytical and numerical density-matrix renormalization group (DMRG) approaches to provide unambiguous conclusions on the nematic state in the J_1–J_2 square-lattice model.

D-wave pair-BEC.—Pairing is ubiquitous in physics [48, 49]. In model (1), the pairing of two spin flips sharing an attractive FM J_1-link occurs in the polarized state. Since the model is 2D, one expects a BS in the s-wave channel for an arbitrarily weak attraction, or any J_2, as in the Cooper problem for superconductivity [48]. Yet, the prior works give a finite J_2-range for the pairing [31, 32] and provide no insight into the pairs' d-wave symmetry.

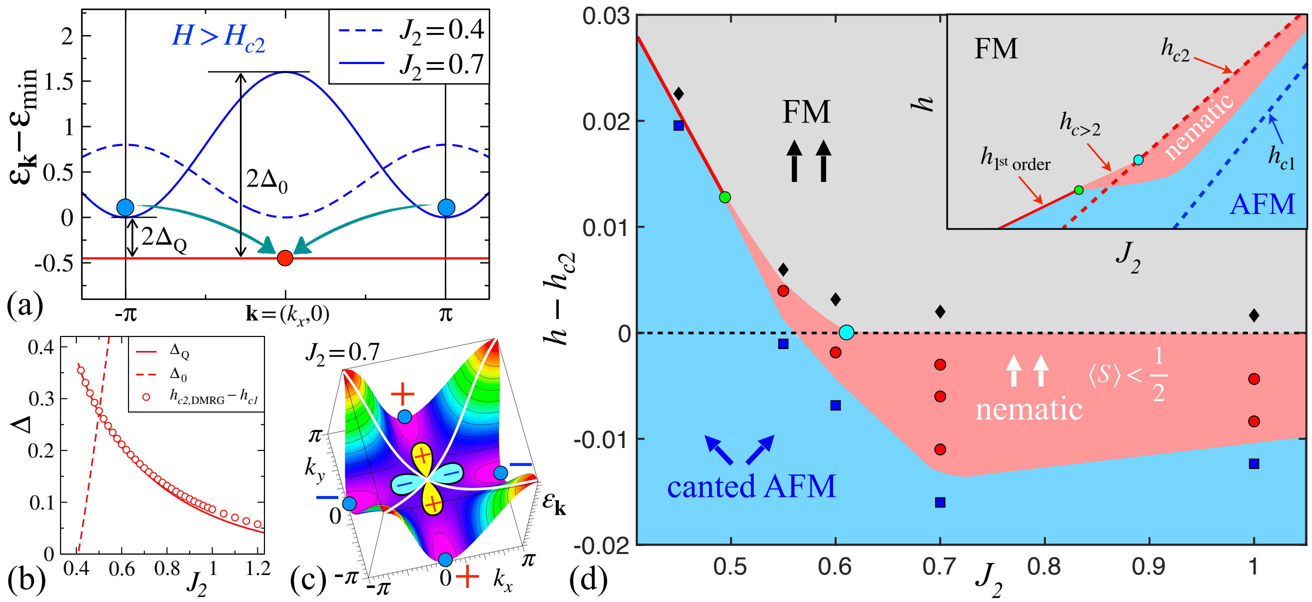

FIG. 2. (a) Magnon energies $\varepsilon_{\mathbf{k}}$ at $h > h_{c2}$ for $J_2 = 0.7$ and 0.4, schematics of magnon pairing, and gaps $\Delta_{\mathbf{Q}(0)}$. (b) The pairing gap Δ vs J_2 from theory (lines) and DMRG (symbols). (c) $\varepsilon_{\mathbf{k}}$ for $J_2 = 0.7$, nodes of the $d_{x^2-y^2}$-wave harmonic (white lines), and schematics of the d-wave. (d) The h–J_2 phase diagram of the model (1) by DMRG, field h is relative to h_{c2}. Symbols mark the FM (black), nematic (red), and AFM (blue) phases. Phase boundaries are inferred from the midpoints between the data. Cyan circle marks a switch to the pair-attraction and green circle to the first-order transition (solid line). Inset: Schematics of the true h–J_2 phase diagram in Fig. 1(b). The nematic region and the deviation from the h_{c2}-line are exaggerated.

The paring of two spin flips can be solved by an exact formalism [29, 41]. It yields the naïve phase diagram of the model (1) shown in Fig. 1(a), where $h_{c1} = 4J_2 - 2$ is the line of the single spin-flip BEC and the FM-AFM border in the classical limit, which is preempted by the pair-BEC at h_{c2} for *any* J_2. DMRG energies for 16×8 cylinders with fixed numbers of spin flips yield h_{c1} and h_{c2} values in nearly-perfect agreement (symbols).

The magnon pairing gap Δ, sketched in Fig. 2(a), is the difference of these fields, $\Delta \equiv h_{c2} - h_{c1}$, which agrees with the weak-coupling result of the Cooper problem [48]

$$\Delta \approx J_2\, e^{-\pi J_2}, \tag{2}$$

for $J_2 \gg 1$, but in the d-wave channel. Fig. 2(c) explains the predominance of the d-wave. The nodes of the $d_{x^2-y^2}$ harmonic of the attraction potential, $V^d_{\mathbf{q}} \propto (\cos q_x - \cos q_y)$, avoid crossing the magnon band minima at $\mathbf{Q} = (0, \pi)[(\pi, 0)]$, see Fig. 2(a), while the nodes of other harmonics do cross them, rendering pairing in these channels unfavorable [50]. The spatial extent of the BS in (2) can be estimated as $\xi \propto \sqrt{J_2/\Delta} \propto e^{\pi J_2/2}$, relating deviations of the DMRG from exact results in Fig. 2(b) at larger J_2 to the finite-size effect [51].

Phase diagram.—With the pairing problem in the FM state solved exactly, its d-wave symmetry and J_2-extent elucidated, a nematic phase is expected to exist below the pair-BEC transition h_{c2} down to the single spin-flip BEC h_{c1}, where the single-particle gap closes and the AFM order prevails, see the phase diagram in Fig. 1(a). However, as we demonstrate, the many-body effects strongly alter some of these expectations, see Figs. 1(b), 1(c), and 2(d).

Generally, for a BEC condensate to form a superfluid phase its constituents must repel [28, 52]. This is the case for the pair-BEC for large (repulsive) J_2, implying that the nematic phase *must* occur in *some* region below the h_{c2}-line, which is unaffected by many-body effects.

As the pair binding energy 2Δ increases for smaller J_2, see Fig. 2(b), one also expects a change of the *pair-pair* interaction from repulsive to attractive. With the numerical evidence for that presented below, this change occurs at about $J_2 \approx 0.6$, marked by a cyan circle in the phase diagrams in Figs. 1(b) and 2(d).

The pair-attraction has two effects. First, the FM-nematic phase boundary in Figs. 2(d) and 1(b) is pulled above the h_{c2}-line, superseded by a BEC of the multi-pair states [53]. Second, the nematic region shrinks as the critical pair density for a transition to the dipolar state is reached more readily. Ultimately, at about $J_2 \approx 0.5$ (green circle in Figs. 2(d) and 1(b)), the nematic phase ceases altogether. In a sense, while the pair-binding gets stronger, the stiffness of the phase vanishes, leading to a first-order collapse of the FM into AFM phase with a finite canting of spins, explaining the zero-field results of Ref. [47] and substantiating the proposal of Ref. [54].

The most striking change concerns the naïve nematic-AFM phase boundary in Fig. 1(a). The h_{c1}-line corresponds to a closing of the single-magnon gap for the non-interacting magnons. However, in the presence of the pair-BEC, this gap is strongly reduced due to attraction to the pair condensate [50], dramatically extending the AFM phase *above* the h_{c1}-line and leading to about an order-of-magnitude contraction of the naïve nematic phase according to DMRG [55]; see Figs. 1 and 2(d).

Our Fig. 2(d) and Figs. 1(b) and 1(c) quantify all of the trends described above: the narrow nematic region below the h_{c2}-line, the change to the pair-attractive regime for $J_2 \lesssim 0.6$ leading to multi-pair transitions and further narrowing of the nematic region, and first-order transition for $J_2 \lesssim 0.5$ together with a shift of the FM-to-AFM boundary from the h_{c2}-line to smaller J_2.

To reveal the resultant phase diagram in Figs. 1(b) and 1(c), we use iterative zooming because the width of the nematic region and the shift of the transition lines are hard to discern on the scale of Fig. 1(a). They are derived from Figure 2(d), which is based on the DMRG results discussed below, with each symbol corresponding to an individual simulation.

DMRG results.—DMRG calculations are performed on the $L_x \times L_y$-site square-lattice cylinders with mixed boundary conditions, and width $L_y = 8$. [56]

We use three complementary approaches. The first is long-cylinder "scans," in which the magnetic field is varied along the length of the 40×8 cylinder, with different phases and their boundaries coexisting in one system. These 1D cuts through the phase diagram are very useful [57–61], allowing one to differentiate first- and second-order transitions by varying the ranges of the scans. Since the parameter gradient can impose unwanted proximity effects, we use such scans judiciously as the first exploratory measure of the nematic phase.

The second approach utilizes 20×8 cylinders, with an aspect ratio that approximates the 2D behavior in the thermodynamic limit [62]. To obtain BEC boundaries in Fig. 1, the pairing gap in Fig. 2(b), and multi-pair energies, we perform calculations for fixed numbers of spin flips (fixed total S^z) as a function of h and J_2.

Lastly, the same cylinders are simulated without fixing total S^z to allow for symmetry-broken phases that are induced by weak edge fields. The broken symmetry allows us to measure local order parameters instead of their correlation functions [57–61]. The decay of the induced orders away from the boundary also serves as an excellent indicator of their stability in the 2D bulk.

Our Figure 3 showcases the described approach and its results for $J_2 = 0.55$ and $h = 0.445$; see the leftmost red circle in Fig. 2(d), just above $h_{c2} = 0.441$ for this value of J_2. Fig. 3(a) shows the spin configuration, with arrows' length equal to the local ordered moment $\langle S\rangle$. In Fig. 3(b) bonds represent the nearest-neighbor pair wave-function $\langle S_i^- S_{i+x(y)}^-\rangle$, which is directly related to the quadrupole-moment order parameter [39], and Fig. 3(c) provides a quantitative measure of them along the length of the cluster. A pairing field $0.1 S_i^- S_{i+y}^-$ (spin-flip field $0.1 S_i^-$) is applied at the left (right) edge.

In order to avoid the pitfalls of the earlier work [31], an important step in the search for the nematics is to rigorously rule out dipolar orders, since nematic correlations also exist in them as a subsidiary of the multipole

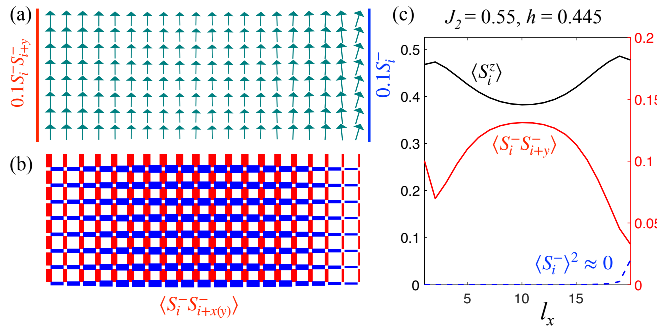

FIG. 3. DMRG results in the 20×8 cluster for $J_2 = 0.55$ and $h = 0.445$. (a) Ordered moment $\langle S\rangle$ in the xz-plane with pairing field $0.1 S_i^- S_{i+y}^-$ (spin-flip field $0.1S_i^-$) at the left (right) edge. (b) Nearest-neighbor component of the pair wave-function; thickness (color) of the bond corresponds to the value (sign) of $\langle S_i^- S_{i+x(y)}^-\rangle$. (c) z-axis magnetization $\langle S_i^z\rangle \approx \langle S\rangle$ (left axis), and nematic $\langle S_i^- S_{i+y}^-\rangle$ and spin-canting $\langle S_i^-\rangle^2$ order parameters (right axis) along the cylinder.

expansion. As one can see in Fig. 3(a) and 3(c), the magnetization is markedly suppressed from full saturation away from the boundary, $\langle S^z\rangle < \frac{1}{2}$, but shows no sign of canting. In the same region, the quadrupolar order parameter is clearly developed, with $\langle S_i^- S_{i+y}^-\rangle \gtrsim 0.1$ and its d-wave character evident from the opposite sign of the horizontal and vertical bonds in Fig. 3(b). On the other hand, the induced canting on the right edge decays away from it with no detectable $\langle S_i^-\rangle$ in the bulk; see Figs. 3(a) and 3(c), which indicate a gap to one-magnon excitations and the absence of the dipolar order.

Altogether, the analysis presented in Fig. 3 leaves no doubt for the presence of the d-wave nematic state for the chosen values of h and J_2. We point out again that without the pinning field, the nematic state still exists and can be detected through the pair-pair correlations instead of the local order parameter, but they are no more informative and less visual than the results in Fig. 3.

In Figure 4, we show a long-cylinder scan for $J_2 = 0.7$ with varied h. From Fig. 1(a) one expects to see the nematic phase from the single-magnon-BEC to the pair-BEC fields, from $h_{c1} = 0.792$ to $h_{c2} = 0.966$. Instead, we observe a robust AFM phase with substantial dipolar order $\langle S_i^-\rangle$ all the way up to a vicinity of h_{c2}; see Figs. 4(a) and 4(b). Although $\langle S^z\rangle$ in Fig. 4(b) drops precipitously in a narrow field range near h_{c2}, varying the limits of the scan suggests second-order transition(s).

Fig. 4(b) shows that near h_{c2} the nematic order parameter dominates the dipolar one, suggesting the presence of the nematic phase. This behavior is markedly different from the case of the quadrupolar order occurring as a byproduct of the dipolar one in the pure AFM model [50]. However, because of the proximity effects of the neighboring phases, it is difficult to make definite conclusions on the extent of the nematic region based solely on the results of Fig. 4(b), besides the fact that it is much narrower than suggested naïvely in Fig. 1(a).

Thus, we carry out the fixed-parameter, 20×8 clus-

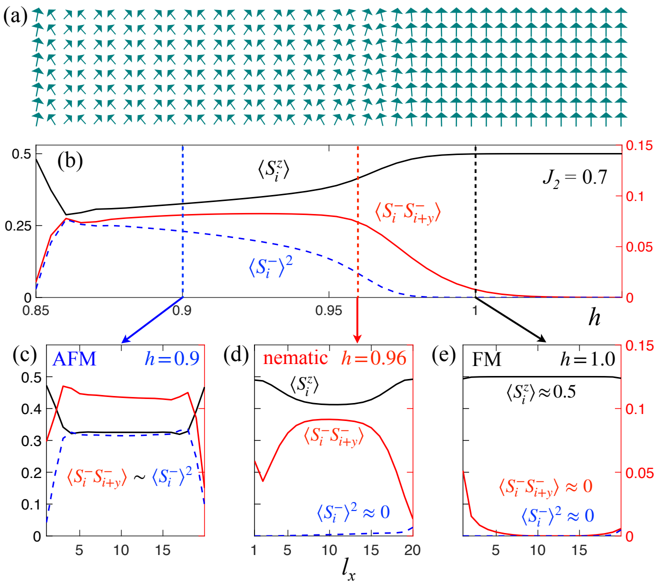

FIG. 4. Long-cylinder scan in h from 0.85 to 1.05 for $J_2 = 0.7$, with (a) spin pattern of the ordered moments (field $0.1S_i^-$ at the left edge), and (b) magnetization $\langle S_i^z\rangle$ (left axis), and pair $\langle S_i^- S_{i+y}^-\rangle$ and spin-canting $\langle S_i^-\rangle^2$ order parameters (right axis). (c), (d) and (e) Fixed-parameter calculations as in Fig. 3(c) for $h = 0.9$, 0.96, and 1.0, respectively.

ter calculation as in Fig. 3 for several values of h along the path of the scan in Fig. 4(b). The results for three such fields, 0.9, 0.96, and 1.0, are shown in Figs. 4(c)-(e). Fig. 4(d) mirrors Fig. 3(c), clearly placing $h = 0.96$ in the nematic region. The finite-size scaling of the nematic order shows little change [50], indicating the near-2D character of our results. The $h = 1.0$ point in Fig. 4(e) shows saturated ordered moment and a decay of both pair and spin-canting away from the boundaries, confirming a polarized FM state. The $h = 0.9$ point in Fig. 4(c) demonstrates a strong presence of both dipolar and quadrupolar orders—a sign of the AFM phase. For all the (J_2, h) data points contributing to the phase diagram in Fig. 2(d), we performed the same type of analysis.

In Figure 5, we present the results of the same analysis for $J_2 = 0.45$, with the scan in h from 0.0 to 0.2. Unlike the case of Figure 4, where the evolution of magnetization suggests second-order transitions, in Fig. 5(a) and 5(b) one can notice that the canting of spins changes to a fully polarized state rather drastically. The transition is at about $h \approx 0.14$, which is also noticeably *higher* than the pair-BEC value of $h_{c2} = 0.12$ from Fig. 1(a). Another feature is the "scale-invariance" of the scan, demonstrated in Fig. 5(c) by zooming on the narrow field range of 0.12 to 0.16, suggesting the first-order character of the transition. The fixed-parameter calculations described above also find no nematic region between the AFM and FM states, supporting our scenario that pair attraction leads to a first-order collapse of the multi-pair state directly into the dipolar instead of the nematic phase, in a broad agreement with the proposal of Ref. [54].

The AFM-FM transition remains first-order down to

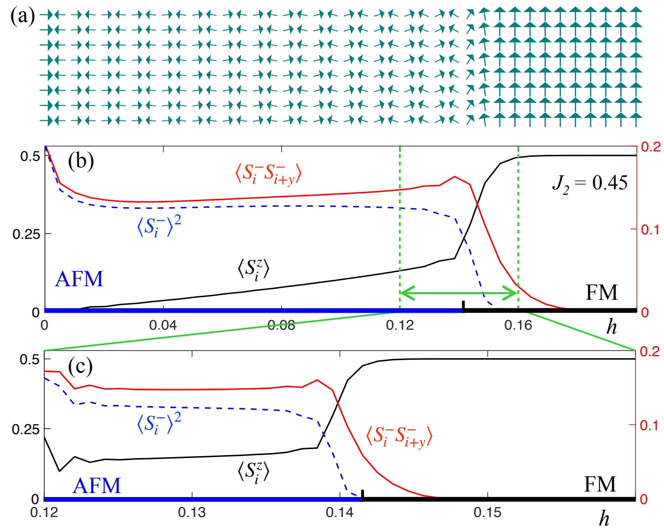

FIG. 5. (a) and (b) Same as (a) and (b) in Fig. 4 for $J_2 = 0.45$ and h from 0.0 to 0.2. (c) Same as (b) for h from 0.12 to 0.16.

zero field with the boundary shifting to $J_2 \approx 0.39$ from the pair-BEC value of $J_2 \approx 0.408$, see Fig. 1(b), in agreement with $J_2 = 0.394$ from the earlier study [47].

Multi-pair states.—For $J_2 \lesssim 0.6$ (left of the cyan circle in Fig. 2), spin-flip pairs attract each other and can form multi-pair states. As a result, the actual transition from the FM phase is above h_{c2} and is into the condensates of these multi-pair states. Furthermore, the quadrupolar nematic phase also extends above the h_{c2} line, see Figs. 2(d) and 1(b), for the same reason the dipolar AFM phase is pulled up above the h_{c1} line.

In the regime associated with the pair-attraction, we identified condensations from the FM phase into the states with four, six, and eight magnons in a 16×8 cluster, see Ref. [50]. They form a devil's staircase of diminishing ranges of J_2 before reaching the first-order transition point at $J_2 \approx 0.5$, bearing a resemblance to the results of Refs. [39, 40]. However, an unambiguous confirmation of the higher-multipolar orders associated with the multi-pair BECs is beyond the present study because of the finite-size effects and weak higher-order pairing.

Summary.—We have established the actual extent of the d-wave nematic phase in the phase diagram of the paradigmatic J_1–J_2 model using analytical and DMRG insights. The nature of the d-wave pairing is explained and the criteria for the existence of the pair-BEC are elucidated. The sequence of the multi-pair BEC transitions is suggested to bridge the d-wave pair-BEC and the first-order FM-AFM transition lines.

The nematic state is not stable at zero field and in the J_2 region close to the FM-AFM border because repulsive pair-pair interactions are generally required to ensure finite stiffness of the pair-BEC state. A suppression of the single-spin-flip gap by an attraction to the pair-condensate is shown to lead to a dramatic order-of-magnitude contraction of the nematic phase compared to the naïve expectations. The hallmark of the remaining nematic region is the significant drop in the magnetization in a very narrow field range near saturation without any dipolar order. Our work provides vital guidance to the ongoing theoretical and experimental searches of the elusive quantum spin-nematics, arming them with realistic expectations. The proposed scenario and the phase diagram can be expected to be valid for a wide variety of models and materials.

Acknowledgments.—The work of S. J. and S. R. W. was supported by the NSF through grant DMR-2110041. The work of J. R. was supported by the NSF through grant DMR-2142554. The work of M. E. Z. was supported by ANR, France, Grant No. ANR-15-CE30-0004. The work of A. L. C. was supported by the U.S. Department of Energy, Office of Science, Basic Energy Sciences under Award No. DE-SC0021221.

[1] P.-G. De Gennes and J. Prost, *The physics of liquid crystals*, 83 (Oxford university press, 1993).
[2] D. Andrienko, Introduction to liquid crystals, J. Mol. Liq. **267**, 520 (2018).
[3] E. Fradkin, S. A. Kivelson, M. J. Lawler, J. P. Eisenstein, and A. P. Mackenzie, Nematic fermi fluids in condensed matter physics, Annu. Rev. Condens. Matter Phys. **1**, 153 (2010).
[4] J.-H. Chu, H.-H. Kuo, J. G. Analytis, and I. R. Fisher, Divergent nematic susceptibility in an iron arsenide superconductor, Science **337**, 710 (2012).
[5] R. M. Fernandes, A. V. Chubukov, and J. Schmalian, What drives nematic order in iron-based superconductors?, Nat. Phys. **10**, 97 (2014).
[6] S. Mukhopadhyay, R. Sharma, C. K. Kim, S. D. Edkins, M. H. Hamidian, H. Eisaki, S. ichi Uchida, E.-A. Kim, M. J. Lawler, A. P. Mackenzie, J. C. S. Davis, and K. Fujita, Evidence for a vestigial nematic state in the cuprate pseudogap phase, Proc. Natl. Acad. Sci. U.S.A. **116**, 13249 (2019).
[7] F. Mila, Closing in on a Magnetic Analog of Liquid Crystals, Physics **10**, 64 (2017).
[8] R. Nath, A. A. Tsirlin, H. Rosner, and C. Geibel, Magnetic properties of $BaCdVO(PO_4)_2$: A strongly frustrated spin-$\frac{1}{2}$ square lattice close to the quantum critical regime, Phys. Rev. B **78**, 064422 (2008).
[9] L. E. Svistov, T. Fujita, H. Yamaguchi, S. Kimura, K. Omura, A. Prokofiev, A. I. Smirnov, Z. Honda, and M. Hagiwara, New high magnetic field phase of the frustrated $S= 1/2$ chain compound $LiCuVO_4$, JETP letters **93**, 21 (2011).
[10] M. Yoshida, K. Nawa, H. Ishikawa, M. Takigawa, M. Jeong, S. Krämer, M. Horvatić, C. Berthier, K. Matsui, T. Goto, S. Kimura, T. Sasaki, J. Yamaura, H. Yoshida, Y. Okamoto, and Z. Hiroi, Spin dynamics in the high-field phases of volborthite, Phys. Rev. B **96**, 180413(R) (2017).
[11] A. Orlova, E. L. Green, J. M. Law, D. I. Gorbunov, G. Chanda, S. Krämer, M. Horvatić, R. K. Kremer, J. Wosnitza, and G. L. J. A. Rikken, Nuclear magnetic resonance signature of the spin-nematic phase in $LiCuVO_4$ at high magnetic fields, Phys. Rev. Lett. **118**, 247201 (2017).
[12] Y. Kohama, H. Ishikawa, A. Matsuo, K. Kindo, N. Shannon, and Z. Hiroi, Possible observation of quantum spin-nematic phase in a frustrated magnet, Proc. Natl. Acad. Sci. U.S.A. **116**, 10686 (2019).
[13] K. Y. Povarov, V. K. Bhartiya, Z. Yan, and A. Zheludev, Thermodynamics of a frustrated quantum magnet on a square lattice, Phys. Rev. B **99**, 024413 (2019).
[14] V. K. Bhartiya, K. Y. Povarov, D. Blosser, S. Bettler, Z. Yan, S. Gvasaliya, S. Raymond, E. Ressouche, K. Beauvois, J. Xu, F. Yokaichiya, and A. Zheludev, Presaturation phase with no dipolar order in a quantum ferro-antiferromagnet, Phys. Rev. Research **1**, 033078 (2019).
[15] F. Landolt, S. Bettler, Z. Yan, S. Gvasaliya, A. Zheludev, S. Mishra, I. Sheikin, S. Krämer, M. Horvatić, A. Gazizulina, and O. Prokhnenko, Presaturation phase in the frustrated ferro-antiferromagnet $Pb_2VO(PO_4)_2$, Phys. Rev. B **102**, 094414 (2020).
[16] K. M. Ranjith, F. Landolt, S. Raymond, A. Zheludev, and M. Horvatić, NMR evidence against a spin-nematic nature of the presaturation phase in the frustrated magnet $SrZnVO(PO_4)_2$, Phys. Rev. B **105**, 134429 (2022).
[17] D. Flavián, S. Hayashida, L. Huberich, D. Blosser, K. Y. Povarov, Z. Yan, S. Gvasaliya, and A. Zheludev, Magnetic phase diagram of the linear quantum ferro-antiferromagnet $Cs_2Cu_2Mo_3O_{12}$, Phys. Rev. B **101**, 224408 (2020).
[18] A. F. Andreev and I. M. Lifshitz, Quantum theory of defects in crystals, Sov. Phys. JETP **29**, 1107 (1969).
[19] A. J. Leggett, Can a Solid Be "Superfluid"?, Phys. Rev. Lett. **25**, 1543 (1970).
[20] J. Léonard, A. Morales, P. Zupancic, T. Esslinger, and T. Donner, Supersolid formation in a quantum gas breaking a continuous translational symmetry, Nature **543**, 87 (2017).
[21] M. A. Norcia, C. Politi, L. Klaus, E. Poli, M. Sohmen, M. J. Mark, R. N. Bisset, L. Santos, and F. Ferlaino, Two-dimensional supersolidity in a dipolar quantum gas, Nature **596**, 357 (2021).
[22] L. Savary and L. Balents, Quantum spin liquids: a review, Rep. Prog. Phys. **80**, 016502 (2016).
[23] J. Knolle and R. Moessner, A field guide to spin liquids, Annual Review of Condensed Matter Physics **10**, 451 (2019).
[24] M. Blume and Y. Y. Hsieh, Biquadratic exchange and quadrupolar ordering, J. Appl. Phys. **40**, 1249 (1969).
[25] A. F. Andreev and I. A. Grishchuk, Spin nematics, Sov. Phys. JETP **60**, 267 (1984).
[26] A. V. Chubukov, Chiral, nematic, and dimer states in quantum spin chains, Phys. Rev. B **44**, 4693 (1991).
[27] K. Penc and A. M. Läuchli, in *Introduction to Frustrated Magnetism: Materials, Experiments, Theory*, edited by C. Lacroix, P. Mendels, and F. Mila (Springer-Verlag Berlin Heidelberg, 2011) Chap. Spin Nematic Phases in Quantum Spin Systems, p. 331.
[28] V. Zapf, M. Jaime, and C. D. Batista, Bose-einstein condensation in quantum magnets, Rev. Mod. Phys. **86**, 563 (2014).
[29] M. Wortis, Bound States of Two Spin Waves in The Heisenberg Ferromagnet, Phys. Rev. **132**, 85 (1963).
[30] D. C. Mattis, *The theory of magnetism made simple: an introduction to physical concepts and to some use-*

ful mathematical methods (WorId Scientific Publishing, Singapore, 2006).
[31] N. Shannon, T. Momoi, and P. Sindzingre, Nematic Order in Square Lattice Frustrated Ferromagnets, Phys. Rev. Lett. **96**, 027213 (2006).
[32] P. Sindzingre, L. Seabra, N. Shannon, and T. Momoi, Phase diagram of the spin-1/2 J_1–J_2–J_3 Heisenberg model on the square lattice with ferromagnetic J_1, J. Phys. Conf. Ser. **145**, 012048 (2009).
[33] Y. Iqbal, P. Ghosh, R. Narayanan, B. Kumar, J. Reuther, and R. Thomale, Intertwined nematic orders in a frustrated ferromagnet, Phys. Rev. B **94**, 224403 (2016).
[34] R. O. Kuzian and S.-L. Drechsler, Exact one- and two-particle excitation spectra of acute-angle helimagnets above their saturation magnetic field, Phys. Rev. B **75**, 024401 (2007).
[35] T. Hikihara, L. Kecke, T. Momoi, and A. Furusaki, Vector chiral and multipolar orders in the spin-$\frac{1}{2}$ frustrated ferromagnetic chain in magnetic field, Phys. Rev. B **78**, 144404 (2008).
[36] T. Momoi, P. Sindzingre, and K. Kubo, Spin Nematic Order in Multiple-Spin Exchange Models on the Triangular Lattice, Phys. Rev. Lett. **108**, 057206 (2012).
[37] R. Shindou and T. Momoi, $SU(2)$ slave-boson formulation of spin nematic states in $S = \frac{1}{2}$ frustrated ferromagnets, Phys. Rev. B **80**, 064410 (2009).
[38] T. Momoi and N. Shannon, Nematic Order in the Multiple-Spin Exchange Model on the Triangular Lattice, Prog. Theor. Phys. **159**, 72 (2005).
[39] J. Sudan, A. Lüscher, and A. M. Läuchli, Emergent multipolar spin correlations in a fluctuating spiral: The frustrated ferromagnetic spin-$\frac{1}{2}$ Heisenberg chain in a magnetic field, Phys. Rev. B **80**, 140402(R) (2009).
[40] L. Balents and O. A. Starykh, Quantum lifshitz field theory of a frustrated ferromagnet, Phys. Rev. Lett. **116**, 177201 (2016).
[41] M. E. Zhitomirsky and H. Tsunetsugu, Magnon pairing in quantum spin nematic, EPL (Europhysics Letters) **92**, 37001 (2010).
[42] H. T. Ueda and K. Totsuka, Magnon Bose-Einstein condensation and various phases of three-dimensonal quantum helimagnets under high magnetic field, Phys. Rev. B **80**, 014417 (2009).
[43] O. Janson, S. Furukawa, T. Momoi, P. Sindzingre, J. Richter, and K. Held, Magnetic Behavior of Volborthite $Cu_3V_2O_7(OH)_2{\cdot}H_2O$ Determined by Coupled Trimers Rather than Frustrated Chains, Phys. Rev. Lett. **117**, 037206 (2016).
[44] R. Bendjama, B. Kumar, and F. Mila, Absence of Single-Particle Bose-Einstein Condensation at Low Densities for Bosons with Correlated Hopping, Phys. Rev. Lett. **95**, 110406 (2005).
[45] C. Knetter, A. Bühler, E. Müller-Hartmann, and G. S. Uhrig, Dispersion and Symmetry of Bound States in the Shastry-Sutherland Model, Phys. Rev. Lett. **85**, 3958 (2000).
[46] K. Totsuka, S. Miyahara, and K. Ueda, Low-Lying Magnetic Excitation of the Shastry-Sutherland Model, Phys. Rev. Lett. **86**, 520 (2001).
[47] J. Richter, R. Darradi, J. Schulenburg, D. J. J. Farnell, and H. Rosner, Frustrated spin-$\frac{1}{2}$ J_1–J_2 Heisenberg ferromagnet on the square lattice studied via exact diagonalization and coupled-cluster method, Phys. Rev. B **81**, 174429 (2010).
[48] J. F. Annett, *Superconductivity, Superfluids and Condensates* (Oxford University Press Inc., New York, 2006).
[49] J. R. Taylor, *Scattering Theory: The Quantum Theory of Nonrelativistic Collisions* (Dover Publications, 2006).
[50] See Supplemental Material at [], which includes Refs. [63–68], for the details on the nematic order parameters, analytical calculations of the pair bound states, and additional DMRG results on the multi-pair states, finite-size scaling, and dipole and quadrupole order parameters.
[51] For example, $\xi \approx 4.8$ for $J_2 = 1.0$ [50].
[52] E. M. Lifshitz and L. P. Pitaevskii, Chapter III – Superfluidity, in *Statistical Physics, v. 2*, edited by L. D. Landau and E. M. Lifshitz (Pergamon Press, Oxford, 1980) pp. 85–140.
[53] The "true" multi-pair states are likely to occupy only a very narrow region below the $h_{c>2}$ phase boundary, while the nematic phase is also pulled above h_{c2}, in analogy to the AFM state that expands above the h_{c1}-line.
[54] H. T. Ueda and T. Momoi, Nematic phase and phase separation near saturation field in frustrated ferromagnets, Phys. Rev. B **87**, 144417 (2013).
[55] In a similar setting, an earlier work has suggested *expansion* of the nematic phase *below* the h_{c1}-line [41], but it neglected attraction effects between the single spin flips and pair BEC.
[56] Calculations are carried out using the ITensor library [69], typically performing 16 sweeps and reaching a maximum bond dimension of about $m = 2000$ to ensure good convergence with a truncation error $< 10^{-6}$. To avoid metastable states, we use different initial spin configurations and compare converged energies to ensure the ground state is reached.
[57] Z. Zhu and S. R. White, Spin liquid phase of the $S = \frac{1}{2}$ J_1–J_2 Heisenberg model on the triangular lattice, Phys. Rev. B **92**, 041105(R) (2015).
[58] Z. Zhu, D. A. Huse, and S. R. White, Weak Plaquette Valence Bond Order in the $S = 1/2$ Honeycomb J_1–J_2 Heisenberg Model, Phys. Rev. Lett. **110**, 127205 (2013).
[59] Z. Zhu, D. A. Huse, and S. R. White, Unexpected z-Direction Ising Antiferromagnetic Order in a Frustrated Spin-1/2 J_1–J_2 XY Model on the Honeycomb Lattice, Phys. Rev. Lett. **111**, 257201 (2013).
[60] Z. Zhu, P. A. Maksimov, S. R. White, and A. L. Chernyshev, Disorder-Induced Mimicry of a Spin Liquid in $YbMgGaO_4$, Phys. Rev. Lett. **119**, 157201 (2017).
[61] Z. Zhu, P. A. Maksimov, S. R. White, and A. L. Chernyshev, Topography of Spin Liquids on a Triangular Lattice, Phys. Rev. Lett. **120**, 207203 (2018).
[62] S. R. White and A. L. Chernyshev, Neél Order in Square and Triangular Lattice Heisenberg Models, Phys. Rev. Lett. **99**, 127004 (2007).
[63] M. Tinkham, *Group Theory and Quantum Mechanics (Dover Books on Chemistry)* (Dover Publications, 2003).
[64] H. Bethe, Zur Theorie der Metalle, Zeitschrift für Physik **71**, 205 (1931).
[65] R. P. Feynman, *Statistical Mechanics: A Set Of Lectures* (CRC Press, Boca Raton, 1998) pp. 198–220.
[66] F. J. Dyson, General theory of spin-wave interactions, Phys. Rev. **102**, 1217 (1956).
[67] V. M. Galitski, B. Karnakov, V. Galitski, and V. I. Kogan, *Exploring Quantum Mechanics: A Collection of 700+ Solved Problems for Students, Lecturers, and Researchers* (OUP Oxford, 2013).
[68] M. E. Zhitomirsky and T. Nikuni, Magnetization curve of

a square-lattice heisenberg antiferromagnet, Phys. Rev. B **57**, 5013 (1998).
[69] M. Fishman, S. R. White, and E. M. Stoudenmire, The ITensor software library for tensor network calculations (2020), arXiv:2007.14822.